Rec 7/24/98
doc -

AFRL-SR-BL-TR-98-

0139

REPORT DOCUMENTATION PAGE

Form Approved
OMB No. 0704-0188

1. AGENCY USE ONLY (Leave blank)	2. REPORT DATE	3. REPORT TYPE AND DATES COVERED
	1.12.98	Final, 11.01.96-10.31.97

4. TITLE AND SUBTITLE
Particulate Systems with Viscous and Viscoelastic Cement: From Contact Laws to Macroscopic Behavior

5. FUNDING NUMBERS
US Air Force Office of Scientific Research
Contract F49620-96-1-0394

6. AUTHOR(S)
Jack Dvorkin

7. PERFORMING ORGANIZATION NAMES(S) AND ADDRESS(ES)
Geophysics Department, Stanford University
Stanford, CA 94305-2215

8. PERFORMING ORGANIZATION REPORT NUMBER

9. SPONSORING / MONITORING AGENCY NAMES(S) AND ADDRESS(ES)
Capt. Michael Chipley
Program Manager, AFOSR/NA
110 Duncan Avenue
Bolling AFB, DC 20332-0001

10. SPONSORING / MONITORING AGENCY REPORT NUMBER

11. SUPPLEMENTARY NOTES

19980210 061

a. DISTRIBUTION / AVAILABILITY STATEMENT
Unlimited

13. ABSTRACT (Maximum 200 words)

The overall objective of the proposed research was to provide a quantitative description of the microstructural, as well as macroscopic mechanical behavior of particulate materials with viscous and viscoelastic intergranular cement. By cement, a material is meant which fills the space between two or more particles at their contacts. The volumetric content of cement in the pore space of an aggregate may vary from zero to 100%.

This objective was achieved by deriving microstructural contact laws for the combination of two elastic spherical grains with viscous cement. A simple and accurate viscoelastic approximation (Cole-Cole model) was found for the rigorous micromechanical solution. The contact law thus obtained was used to calculate the effective elastic moduli of a granular aggregate with viscous cement at a varying frequency of oscillations. The theoretical results were verified by experiments conducted on a pack of glass beads with viscous epoxy cement. Our second achievement was the extension of an exact solution for the elastic moduli of a cemented grain pack at a low cement content to a solution for the case where cement occupies the entire pore space or a large portion of it.

The main relevance to the Air Force mission is through a quantitative description of cemented geomaterials such as asphalt cement. The results have been used at the Wright Laboratory to model asphalt concrete's behavior.

14. SUBJECT TERMS			16. NUMBER OF PAGES
Particulate materials, cementation, micromechanics, constitutive laws			35
			16. PRICE CODE
17. SECURITY CLASSIFICATION OF REPORT	18. SECURITY CLASSIFICATION OF THIS PAGE	19. SECURITY CLASSIFICATION OF ABSTRACT	20. LIMITATION OF ABSTRACT
Unclassified	Unclassified	Unclassified	UL

Particulate Systems with Viscous and Viscoelastic Cement: From Contact Laws to Macroscopic Behavior

US AIR FORCE OFFICE OF SCIENTIFIC RESEARCH
CONTRACT F49620-96-1-0394

FINAL REPORT

PI DR. JACK DVORKIN

Geophysics Department, Stanford University
Stanford, CA 94305-2215
Tel. (650) 725-9296
Fax. (650) 725-7344
E-mail jack@pangea.stanford.edu

Stanford, January 1998

1. SUMMARY

1.1. OBJECTIVE AND ACCOMPLISHMENTS

The overall objective of the proposed research was to provide a quantitative description of the microstructural, as well as macroscopic mechanical behavior of particulate materials with viscous and viscoelastic intergranular cement. By cement, a material is meant which fills the space between two or more particles at their contacts. The volumetric content of cement in the pore space of an aggregate may vary from zero to 100%.

This objective was achieved by deriving microstructural contact laws for the combination of two elastic spherical grains with viscous cement. A simple and accurate viscoelastic approximation (Cole-Cole model) was found for the rigorous micromechanical solution. The contact law thus obtained was used to calculate the effective elastic moduli of a granular aggregate with viscous cement at a varying frequency of oscillations. The theoretical results were verified by experiments conducted on a pack of glass beads with viscous epoxy cement.

Our second achievement was the extension of an exact solution for the elastic moduli of a cemented grain pack at a low cement content to a solution for the case where cement occupies the entire pore space or a large portion of it. The theoretical estimates accurately mimic the experimental elastic-wave velocity measurements on artificial and natural granular cemented materials.

The main relevance to the Air Force mission is through a quantitative description of cemented geomaterials such as asphalt cement. The results have been used at the Wright Laboratory to model asphalt concrete's behavior.

1.2. PERSONNEL SUPPORTED

Senior Personnel: Dvorkin, Jack, PI (US). Ph.D. Students: Ran Bachrach (non-US); Amy Day-Lewis (US); Doron Galmudi (non-US); Mike Helgerud (US); Yuguang Liu (non-US); James Packwood (US); Li Teng (non-US).

1.3. PUBLICATIONS

1. Jack Dvorkin, Mickaele Le Ravalec, Jim Berryman, and Amos Nur, 1997, Effective moduli of particulates with elastic cement, submitted to Mechanics of Materials.
2. Klaus C. Leurer and Jack Dvorkin, 1997, Intergranular Squirt Flow in Sand: Grains with Viscous Cement, submitted to Int J. Solids. Struct.

1.4. INTERACTIONS AND TRANSITIONS

Workshops and Conferences:

- 1st Stanford Annual Gas Hydrate Workshop; Stanford, CA, 1997: Modeling Hydrate-Cemented Sands.
- 1997 Stanford Rock Physics Meeting; Stanford, CA, 1997: Natural Cemented Rocks.
- Invited Lecture at Mobil Technical center in Dallas, 1997: Cemented Rocks.
- McNU 1997 Conference: Transition From High-Porosity to Filled Particulates: Effective Medium Modeling.

Transitions:

- USAF Laboratories: Wright Laboratory, Tyndall AFB, Dr. Han Zhu -- used the cementation theory (viscoelastic cement) to describe the deformation of asphalt concrete.

1.6. PATENTS AND INVENTIONS

No patents or inventions resulted form this effort.

2. TECHNICAL PART

In this part the technical results are presented in the form of journal articles. The numeration of formulas and figures is internal for every section.

2.1. INTERGRANULAR SQUIRT FLOW IN SAND: VISCOUS CEMENT

SUPPORTED IN PART BY THE NAVAL RESEARCH LABORATORY

ABSTRACT

We obtained an exact solution to the problem of deformation of two elastic spherical particles with viscous cement at their contact. This model is intended to mimic granular marine sediment whose grains are covered with viscous fluid of geologic (clay suspension) or biogenic nature. It is generally applicable to a granular aggregate with viscous cement. The solution for the normal stiffness of a two-grain combination is reduced to an ordinary integro-differential equation that has to be solved numerically. Based on the numerical solution, we found two approximate expressions for the normal stiffness of a two-grain combination. The first approximation based on the Maxwell viscoelastic model is not very accurate. The second approximation based on the Cole-Cole model is very accurate and can be used instead of the numerical solution. The effective elastic moduli of the aggregate can be calculated using statistical averaging for a dense random pack of identical spheres. The theoretical results match well experimental data obtained on a glass bead pack with viscous epoxy cement.

INTRODUCTION AND PROBLEM FORMULATION

The elastic properties of a granular aggregate such as oil sand or marine sediment strongly depend on the stiffness of the grain-to-grain contacts. The stiffness of the contact region can be affected by the presence of high-viscosity fluid (e.g., heavy oil, clay suspension, or a biogenic material) that envelops the grains. This fluid may act as contact cement by reinforcing the intergranular contacts (Figure 1).

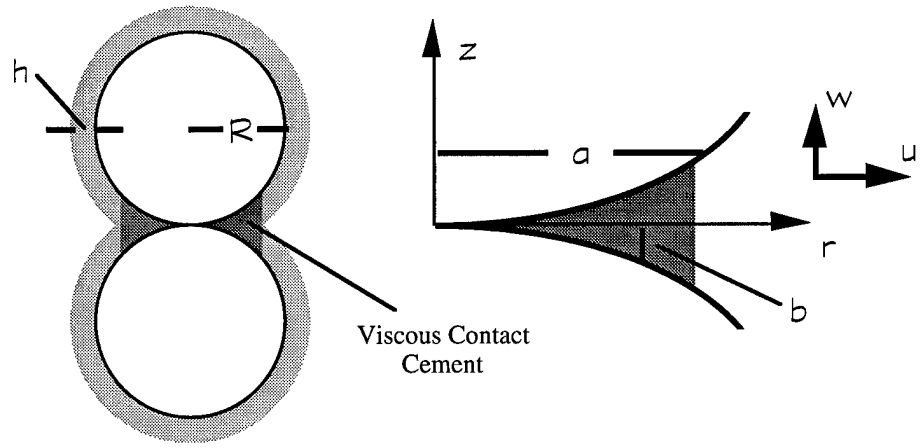

Figure 1. Left: two spherical grains enveloped by high-viscosity fluid. Right: the grain contact region with viscous contact cement.

The effective elastic properties of a granular aggregate with viscous cement are frequency-dependent. At a low frequency, hydrodynamic pressure in viscous cement will be at equilibrium with the surrounding pore space. Therefore, viscous cement will not contribute to the stiffness of the grain-to-grain contact. At a very high frequency, viscous cement becomes unrelaxed and deforms as an elastic body. Now it may strongly reinforce the contacts. At intermediate frequencies local (squirt) flow of viscous cement develops between the grains. This viscous flow is responsible for velocity-frequency dispersion and attenuation. Our goal is to quantitatively describe the squirt flow of viscous cement and understand how it affects the stiffness of the sediment frame and, therefore, acoustic velocity and attenuation in the sediment.

In order to solve the problem, we assume that the grains are spherical and elastic, and cement is a Newtonian compressible viscous fluid. The main part of the solution is finding the normal stiffness of a two-grain combination. This normal stiffness is defined as the ratio of the applied (to the grains) normal force to the resulting increment of the displacement of the sphere center. We assume that the shear stiffness of this combination is non-existent. Also, we assume that the effective pressure acting on the grains is zero, i.e., the direct grain-to-grain contact is a point and the grains are in close-pack suspension.

Once the expression for the normal contact stiffness is obtained, it can be used in a numerical discrete element code. For a special case of a random close pack of identical spherical grains the following analytical expressions can be used to calculate the effective bulk (K_{Eff}) and shear (G_{Eff}) moduli of the aggregate (e.g., Dvorkin et al., 1994):

$$K_{Eff} = \frac{n(1-\phi)}{12\pi R} S_n, \quad G_{Eff} = \frac{3}{5} K_{Eff}; \tag{1}$$

where S_n is the normal stiffness between two grains; $n \approx 9$ is the coordination number (the average number of contacts per grain); $\phi \approx 0.36$ is the aggregate's porosity.

GOVERNING EQUATION

We describe the dynamics of the viscous cement by examining its viscous flow induced by the oscillations of the grain surfaces (Dvorkin et al., 1990). Specifically, we consider oscillations at a fixed angular frequency ω. Then the thickness b of the cement layer in the vicinity of the point grain-to-grain contact is a function of the radial coordinate r and time t:

$$b(r,t) = \frac{r^2}{2R} + b_0(r)e^{i\omega t}, \tag{2}$$

where R is the grain radius, and $b_0 << b$ is the amplitude of the grain surface oscillations.

For an acoustic compressible fluid with the speed of sound c_0 the pressure increment dP is proportional to the density increment $d\rho$ as

$$dP = c_0^2 d\rho. \tag{3}$$

The mass conservation equation in the contact region (Figure 1) is

$$\frac{\partial \rho}{\partial t} + \frac{\partial(\rho u)}{\partial r} + \frac{\rho u}{r} + \frac{\partial(\rho w)}{\partial z} = 0, \tag{4}$$

where u is the velocity component along the r coordinate, and w is the velocity component along the z coordinate.

Let us integrate equation (4) in the z direction from 0 to b and take into account that

$$w = 0, z = 0; \quad w = \frac{\partial b}{\partial t}, z = b. \tag{5}$$

Then

$$\frac{\partial(b\rho)}{\partial t} + \int_0^b [\frac{\partial(\rho u)}{\partial r} + \frac{\rho u}{r}] dz = 0. \tag{6}$$

The approximate Navier-Stokes equation for the radial flow in the contact gap is

$$\frac{\partial u}{\partial t} = -\frac{1}{\rho}\frac{\partial P}{\partial r} + \eta \frac{\partial^2 u}{\partial z^2}, \tag{7}$$

where η is the kinematic viscosity. A solution of equation (7) in the frequency domain is

$$u(r,z) = -\frac{1}{i\omega\rho}\frac{\partial P}{\partial r}[1 - \frac{\cosh(z\sqrt{i\omega/\eta})}{\cosh(b\sqrt{i\omega/\eta})}]. \tag{8}$$

We assume that viscous cement is acoustic fluid and thus variations of density are small as compared to its reference value. Then, and using equations (2) and (3), we have

$$\frac{\partial(\rho u)}{\partial r} \approx \rho \frac{\partial u}{\partial r}, \quad \frac{\partial(\rho b)}{\partial t} \approx \rho \frac{\partial b}{\partial t} + \frac{b}{c_0^2}\frac{\partial P}{\partial t} = i\omega b_0 e^{i\omega t} + i\omega e^{i\omega t}\frac{b}{c_0^2}P. \tag{9}$$

Finally, we substitute equation (8) into (6) and use equations (2) and (9) to obtain an ordinary differential equation for pressure P in the frequency domain:

$$(\frac{\partial^2 P}{\partial r^2} + \frac{\partial P}{r\partial r})(1 - \frac{\tanh\lambda}{\lambda}) + 2\frac{\partial P}{r\partial r}\tanh^2\lambda + P\frac{\omega^2}{c_0^2} = -\omega^2\rho b_0\frac{2R}{r^2}, \tag{10}$$
$$\lambda = (r^2/2R)\sqrt{i\omega/\eta}.$$

In order to find $b_0(r)$ we examine the elastic deformation of the grain surface. We use the following compatibility equation among $b_0(r)$, the displacement $V(r)$ of the grain

surface in the z direction, and the displacement δ of the sphere center (Dvorkin et al, 1994):

$$b_0(r) = V(r) - \delta. \tag{11}$$

Then we use an integral equation that relates $V(r)$ to pressure $P(r)$ in the viscous flow that is exerted upon the grain surface in the contact region (Timoshenko and Goodier, 1970):

$$V(r) = \frac{1-\nu}{\pi G}\int_0^{\pi} d\varphi \int_0^{r\cos\varphi+\sqrt{a^2-r^2\sin^2\varphi}} P(\sqrt{r^2+s^2-2rs\cos\varphi})ds, \tag{12}$$

where ν and G are the grain Poisson's ratio and shear modulus, respectively; and a is the radius of the contact region (Figure 1). This radius is related to the thickness h of the layer of the viscous fluid around the grain as

$$a = \sqrt{2hR}. \tag{13}$$

The integration domain in equation (12) is shown in Figure 2.

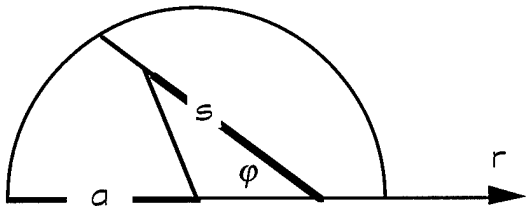

Figure 2. Integration domain in equation (12).

Now by combining equations (10), (11), and (12), we arrive at the governing equation for pressure P:

$$\begin{aligned}&(\frac{\partial^2 P}{\partial r^2}+\frac{\partial P}{r\partial r})(1-\frac{\tanh\lambda}{\lambda})+2\frac{\partial P}{r\partial r}\tanh^2\lambda+P\frac{\omega^2}{{c_0}^2}=\\&-\omega^2\rho\frac{2R}{r^2}[\frac{1-\nu}{\pi G}\int_0^{\pi} d\varphi \int_0^{r\cos\varphi+\sqrt{a^2-r^2\sin^2\varphi}} P(\sqrt{r^2+s^2-2rs\cos\varphi})ds-\delta].\end{aligned} \tag{14}$$

The boundary conditions for equations (10) and (14) are zero pressure fluctuation (from the ambient hydrostatic pressure) at the open boundary of the viscous cement layer, and no

flow at the center of the layer. The expressions for these boundary conditions are, respectively:

$$P = 0, r = a; \quad \frac{dP}{dr} = 0, r = 0. \tag{15}$$

NUMERICAL SOLUTION

To solve equation (14) numerically we first normalize it by introducing the following notations:

$$f = \frac{P}{\rho c_0^{\,2}}, \xi = \frac{s}{R}, x = \frac{r}{R}, \alpha = \frac{a}{R}, \gamma = \frac{c_0}{R\omega}, \lambda = \frac{x^2}{2}\sqrt{\frac{iR^2\omega}{\eta}}, C = \frac{2\delta}{R}.$$

The resulting equation is:

$$\gamma^2(1-\frac{\tanh\lambda}{\lambda})x^2\frac{\partial^2 f}{\partial x^2} + \gamma^2 x(1-\frac{\tanh\lambda}{\lambda}+2\tanh^2\lambda)\frac{\partial f}{\partial x} + x^2 f = -\frac{2\rho c_0^{\,2}(1-\nu)}{\pi G}\int_0^{\pi} d\varphi \int_0^{x\cos\varphi+\sqrt{\alpha^2-x^2\sin^2\varphi}} f(\sqrt{x^2+\xi^2-2x\xi\cos\varphi})d\xi + C. \tag{16}$$

In order to find the desired normal stiffness between two grains we relate the force acting on the grain to displacement δ. Then

$$S_n = \frac{\int_0^a P(r)2\pi r dr}{\delta} = \frac{4\pi R\rho c_0^{\,2}}{C}\int_0^{\alpha} f(x)x dx. \tag{17}$$

It is clear now that equation (16) can be solved with an arbitrarily chosen non-zero C. The resulting normal stiffness will not depend on this choice. We solve equation (16) using the quadrature method (e.g., Delves and Mohamed, 1985).

The results of solving equations (16) and (17) with input parameters G = 45 GPa; ν = 0.064; c_0 = 1500 m/s; ρ = 1 g/cc; R = 10^{-4} m; h = 10^{-7} m; n = 9; ϕ = 0.36; and cement

viscosity 1 cPs; 10^2 cPs; and 10^4 cPs are given (in terms of the real and imaginary parts of the normal stiffness S_n) in Figure 3. The transition zone (from the low-frequency to high-frequency limit) of the real part of S_n as well as the peak of the imaginary part of S_n move up the frequency axis as viscosity of cement decreases. The frequency of this transition is inversely proportional to cement viscosity.

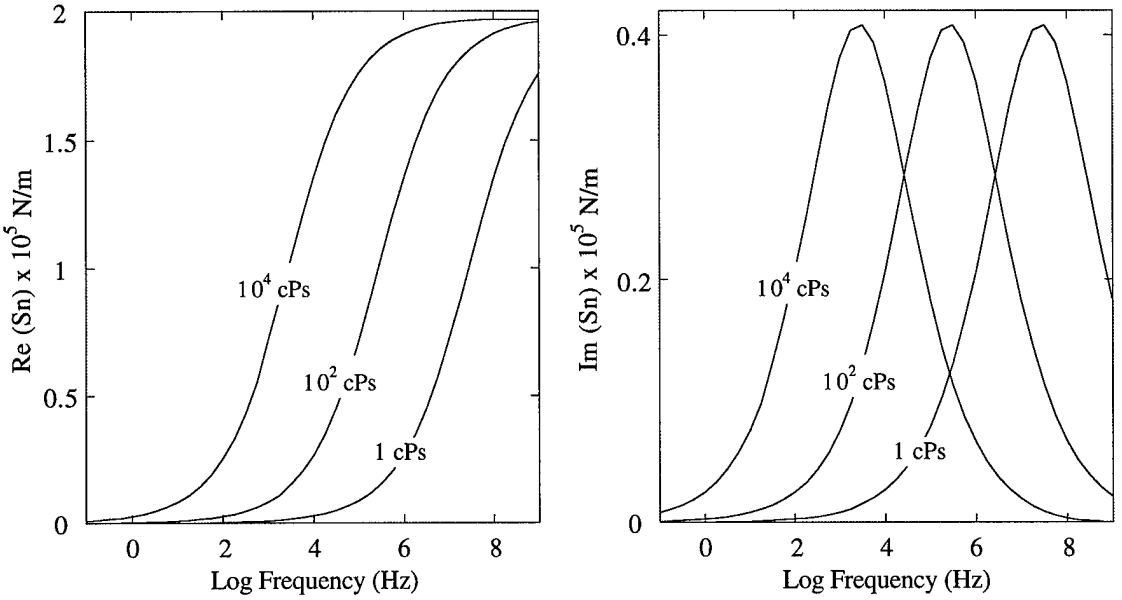

Figure 3. Real and imaginary parts of the normal stiffness versus frequency. The viscosity of cement is given in the plots.

Once S_n is available, we can calculate the effective bulk and shear moduli of the aggregate using equations (1). We stress that equations (1) have been derived for the case of static deformation of a granular aggregate. In the case under consideration the response of the aggregate to the load is clearly time-dependent (Figure 3). Moreover, the imaginary part of this response has the same order of magnitude as the real part. This fact calls for a special non-static analysis of this case. We will address this issue in future work. As of now, we assume that equations (1) are applicable to the case under examination.

IMPLICATIONS OF SOLUTION

We use equations (1) to find the effective bulk and shear moduli of the cemented aggregate, and then equations

$$V_p = \sqrt{\frac{\mathrm{Re}(K_{Eff} + \frac{4}{3} G_{Eff})}{\rho_{Eff}}}, V_s = \sqrt{\frac{\mathrm{Re}(G_{Eff})}{\rho_{Eff}}}, \tag{18}$$

where ρ_{Eff} is the bulk density of the aggregate, to calculate compressional- and shear-wave velocities V_p and V_s. The grain density in these calculations was 2.65 g/cc (quartz).

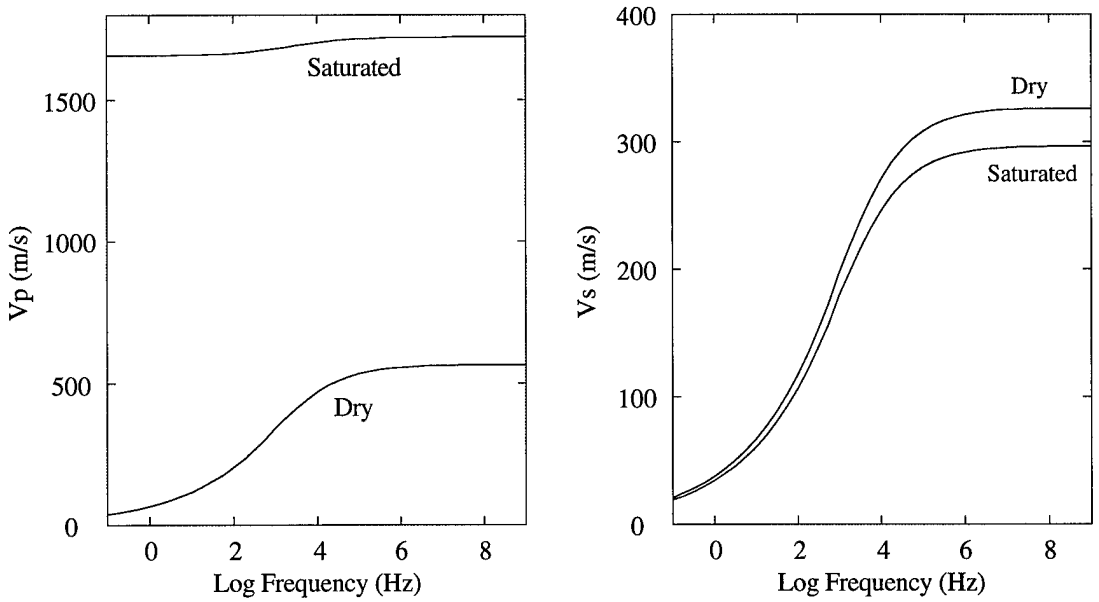

Figure 4. P- and S-wave velocity versus frequency for dry frame and saturated sediment.

Equation (18) gives wave velocities for the dry cemented frame of marine sediment. In order to calculate these velocities in the water-saturated sediment, we use Gassmann's (1951) equation whose applicability to the case under examination (see discussion at the end of the previous section) will be investigated later. The result for cement viscosity 10^4 cPs and the saturating fluid being pure water are given in Figure 4. The blow-ups for P-wave velocity are given in Figure 5.

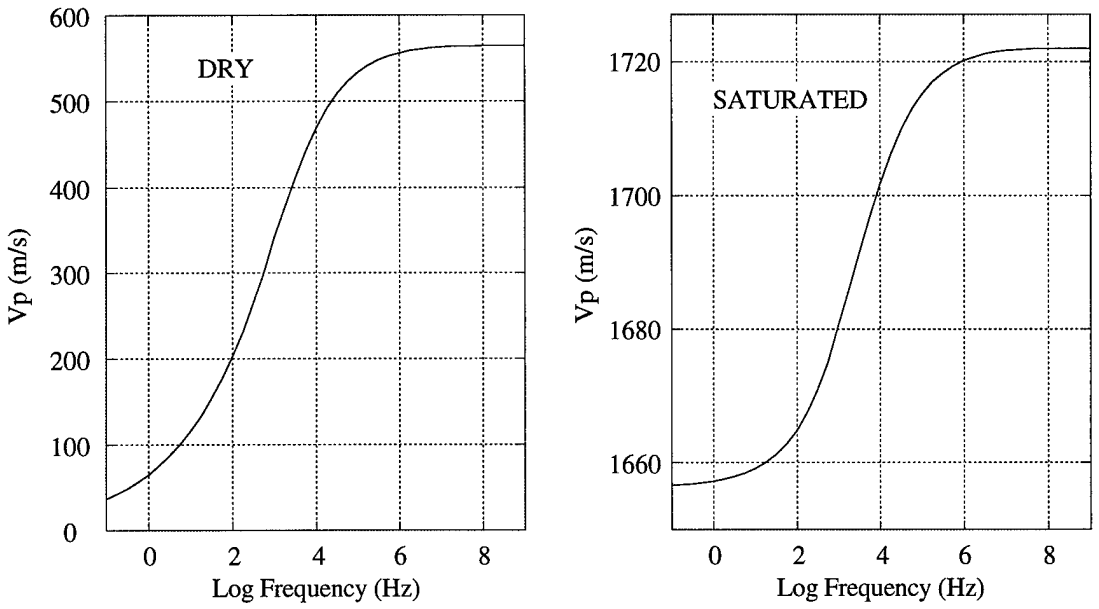

Figure 5. P- wave velocity versus frequency for dry frame and saturated sediment (blowup).

APPROXIMATE SOLUTION: MAXWELL BODY

By carrying out the exact numerical solution for the normal stiffness in a wide range of input parameters, we find the following approximate expressions:

$$\frac{\mathrm{Re}(S_n)}{2\pi R\rho {c_0}^2} = S_\infty \frac{\omega^2\tau^2}{1+\omega^2\tau^2}; \quad \frac{\mathrm{Im}(S_n)}{2\pi R\rho {c_0}^2} = S_\infty \frac{\omega\tau}{1+\omega^2\tau^2}; \tag{19}$$

where

$$\begin{aligned} &S_\infty = \tilde{A}\alpha^2 + \tilde{B}\alpha + \tilde{C}; \\ &\tilde{A} = 19.7472\cdot\exp(-51.9238\Lambda),\ \tilde{B} = 0.795673\cdot\Lambda^{-0.365617}, \\ &\tilde{C} = -0.00391064\cdot\Lambda^{-0.583262};\ \Lambda = \rho {c_0}^2(1-\nu)/(\pi G);\ \tau = 0.8\sqrt{2}\eta/(\alpha^3 {c_0}^2). \end{aligned} \tag{20}$$

Equations (19) describe a Maxwell body (e.g., Bourbie et al., 1987) with the following constitutive equation:

$$\frac{d\delta}{dt} = \frac{F}{\mu} + \frac{1}{E}\frac{dF}{dt}, \tag{21}$$

where F is the contact force and δ is the corresponding displacement; and viscoelastic constants μ and E are:

$$E = 2\pi R\rho c_0^{\,2} S_\infty, \quad \mu = 2\pi R\rho c_0^{\,2} S_\infty \tau. \tag{22}$$

This approximate solution is compared to the exact numerical solution in Figure 6. The high-frequency and low-frequency end members of the exact and approximate solutions are very close to each other, however, the amplitude of the imaginary part of the approximate solution is about twice that of the exact solution. The reason is that in the Maxwell body model we use a single relaxation time which results in a narrow (in the frequency domain) transition region from the low-frequency behavior to the high-frequency behavior.

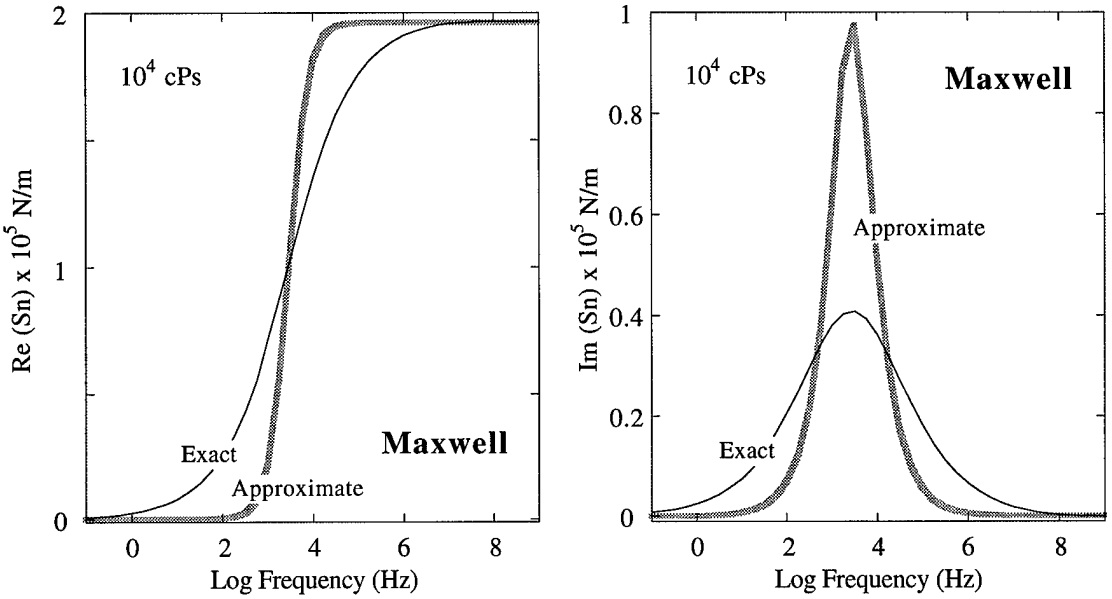

Figure 6. Real and imaginary parts of the normal stiffness versus frequency, exact and approximate Maxwell solutions. The viscosity of cement is given in the plots.

APPROXIMATE SOLUTION: COLE-COLE MODEL

A much better (than the Maxwell body) approximation to our exact numerical solution is given by the Cole-Cole (1941) model:

$$\frac{\mathrm{Re}(S_n)}{2\pi R\rho c_0^{\,2}} = S_\infty\left(1 - \frac{1+\sqrt{\omega\tau/2}}{1+\sqrt{2\omega\tau}+\omega\tau}\right);$$
$$\frac{\mathrm{Im}(S_n)}{2\pi R\rho c_0^{\,2}} = S_\infty \frac{\sqrt{\omega\tau/2}}{1+\sqrt{2\omega\tau}+\omega\tau}. \tag{23}$$

The results of this approximation are compared with the exact solution in Figure 7.

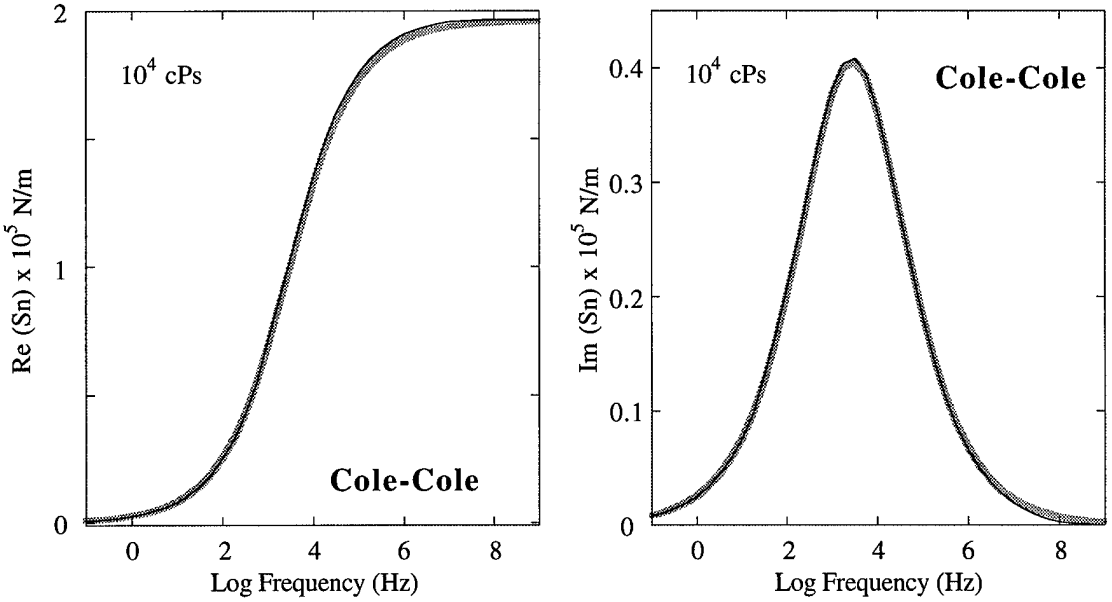

Figure 7. Real and imaginary parts of the normal stiffness versus frequency, exact (thin dark curve) and approximate Cole-Cole (bold gray curve) solutions. The viscosity of cement is given in the plots.

EXPERIMENTAL VERIFICATION OF RESULTS

We apply our theoretical model to reproduce ultrasonic (1 MHz) experimental P-wave velocity measurements conducted on a dense random pack of identical glass beads partially saturated with liquid epoxy. The measurements have been conducted at finite confining pressure values since it was impossible (due to coupling problems) to propagate a pulse through the system at zero confining pressure. Our theoretical model, on the other hand, assumes that the grains are not precompacted.

To apply our model to the system used in the experiments, we modify it by assuming that an elastic spring is placed in parallel to the original viscoelastic model. This spring represents the finite stiffness of the system without epoxy present. As a result, we can determine the stiffness of the spring using velocity measurements at zero epoxy saturation. Then, in order to convert the experimental measurement results at a confining pressure to

those without confinement, we have to subtract the elastic modulus of the dry system from that at a finite epoxy saturation.

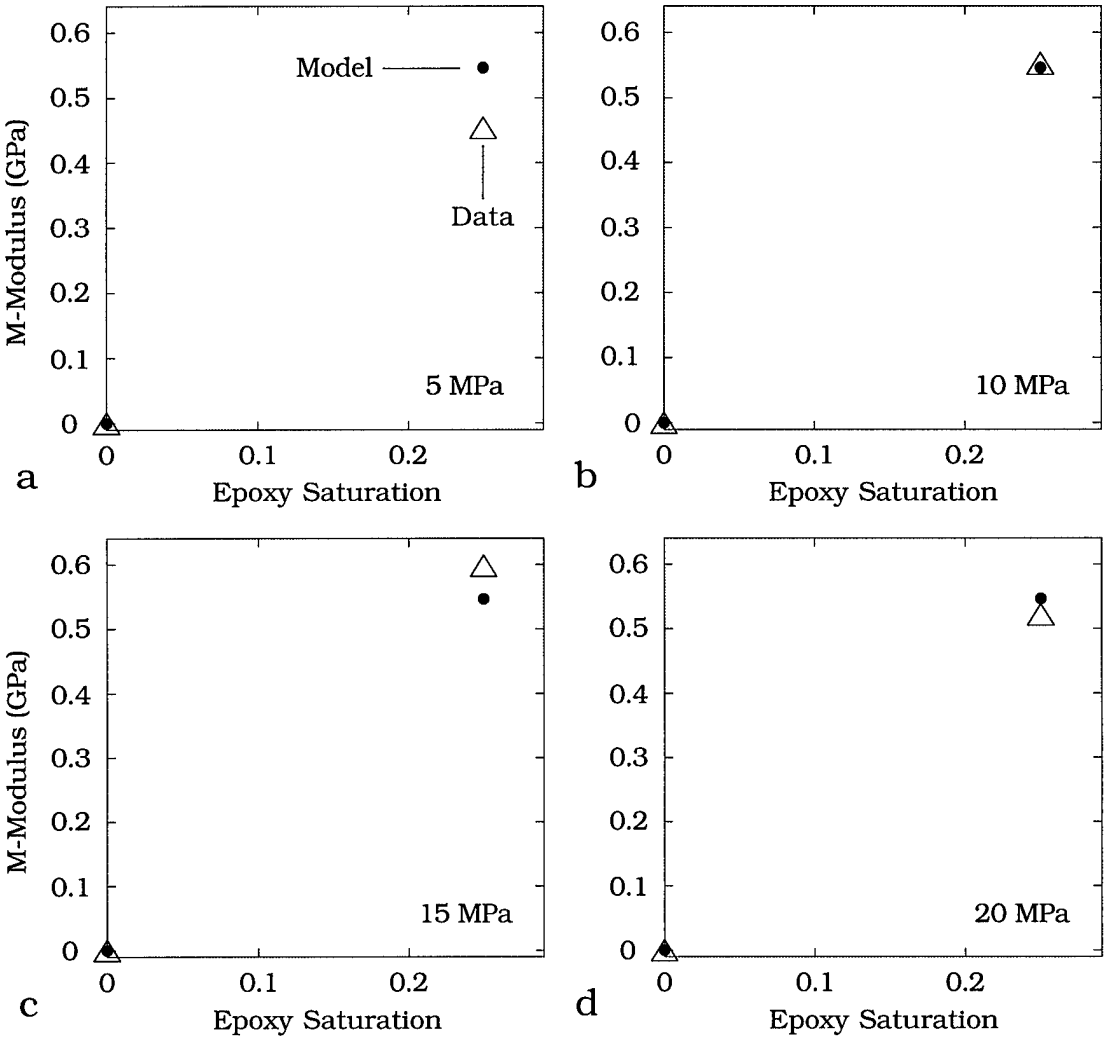

Figure 8. Compressional-wave modulus (M -modulus) difference (saturated minus dry) of a glass-bead pack versus epoxy saturation. Filled circles are the data, triangles are from our model.

We have available velocity measurements 5, 10, 15, and 20 MPa confining pressure in a dry glass bead pack and in the pack with 25% epoxy saturation (Yin, 1993). In order to reproduce the experiment, we assume that the shear modulus, Poisson's ratio, and density of glass are 26.2 GPa, 0.277, and 2.48 g/cm^3, respectively (Dvorkin et al., 1994).

We did not have direct data for the viscosity, density, and the acoustic velocity in pure epoxy. We selected reasonable values of 200 cPs, 1500 m/s, and 1 g/cm^3, respectively (Yin, 1993). These values allow us to consistently match the experimental data at all confining pressures (Figure 8) which confirms the validity of our theoretical model.

In these calculations, we assumed that the epoxy evenly envelopes every grain. Therefore, the normalized contact radius α can be related to epoxy saturation s_E as (Dvorkin and Nur, 1996)

$$\alpha = \sqrt{s_E \frac{2\phi}{3(1-\phi)}}. \tag{24}$$

RELATING ELASTIC MODULI TO POROSITY

The above results are appropriate for modeling the elastic response of an unconsolidated sediment at about 36% porosity, which is the porosity of a random pack of identical spheres (critical porosity -- Nur et al., 1991). In order to extend this result for the entire porosity range, we use a model of Dvorkin et al. (1998) where the Hashin-Shtrikman bounds are used to calculate the dry-frame elastic moduli from those at the critical porosity. For porosity ϕ below critical porosity ϕ_c, we have

$$\begin{aligned} K_{Dry}(\phi) &= \left[\frac{\phi/\phi_c}{K_{Eff}+\frac{4}{3}G_{Eff}} + \frac{1-\phi/\phi_c}{K+\frac{4}{3}G_{Eff}}\right]^{-1} - \frac{4}{3}G_{Eff}, \\ G_{Dry}(\phi) &= \left[\frac{\phi/\phi_c}{G_{Eff}+Z} + \frac{1-\phi/\phi_c}{G+Z}\right]^{-1} - Z, \quad Z = \frac{G_{Eff}}{6}\left(\frac{9K_{Eff}+8G_{Eff}}{K_{Eff}+2G_{Eff}}\right); \quad \phi < \phi_c, \end{aligned} \tag{25}$$

where K_{Eff} and G_{Eff} come from equation (1) using our sphere pack model; and K and G are the bulk and shear moduli of the mineral phase, respectively. For porosity above critical porosity we have

$$K_{Dry} = [\frac{(1-\phi)/(1-\phi_c)}{K_{Eff} + \frac{4}{3}G_{Eff}} + \frac{(\phi-\phi_c)/(1-\phi_c)}{\frac{4}{3}G_{Eff}}]^{-1} - \frac{4}{3}G_{Eff},$$
$$G_{Dry} = [\frac{(1-\phi)/(1-\phi_c)}{G_{Eff} + Z} + \frac{(\phi-\phi_c)/(1-\phi_c)}{Z}]^{-1} - Z, \quad \phi > \phi_c. \tag{26}$$

The dry-frame moduli are plotted versus porosity in Figure 9 where the parameters used are the same as for plots in Figure 4, and frequency is infinite (elastic limit).

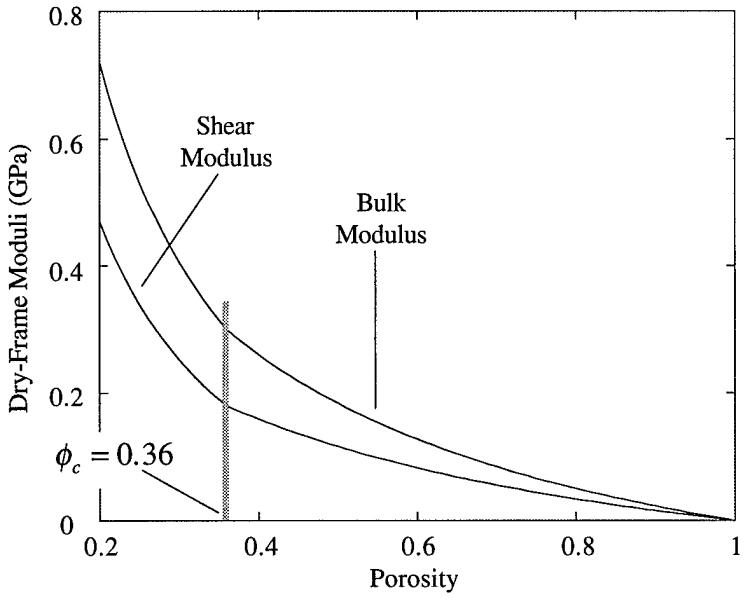

Figure 9. Dry-frame bulk and shear moduli versus porosity calculated using equation (25) and (26).

CONCLUSION

The theoretical model offered here is a first step towards rigorously describing the visco-elastic behavior of a particulate system with viscous cement at grain contacts. Such systems may be encountered in nature (marine sediments with clay and/or biogenic viscous matter enveloping the grains; heavy oil sands; shallow sands with viscous contaminant) and in engineering applications (asphalt concrete). The model developed here is strictly speaking appropriate only for describing suspensions with zero effective pressure. Our next step is to extend this model for the case where the contacting grains are subject to a finite confining force and thus have a direct contact (Hertzian) area rather than a point.

Such theoretical development will be accompanied by pulse-transmission experiments to measure elastic-wave velocities in relevant granular systems.

Another goal is to find an appropriate physical representation for the Cole-Cole model employed here that can be easily used in a numerical discrete element code.

In calculating the elastic moduli of the fully saturated system, we used Gassmann's equation where the dry-frame moduli are given by our model for a pack with viscous cement. We did so for simplicity. However, it is straightforward to use the Biot model instead which may help account for the global frequency dispersion in the system.

REFERENCES

Bourbie, T., Coussy, O., and Zinszner, B., 1987, Acoustics of porous media: Gulf Publishing Co.

Cole, S., and Cole, R.H., 1941, Dispersion and absorption in dielectrics: J. Chem. Phys., 9, 341-351.

Delves, L.M., and Mohamed, J.L., 1985, Computational methods for integral equations: Cambridge University Press.

Dvorkin, J., Mavko, G., and Nur, A., 1990, The oscillations of a viscous compressible fluid in an arbitrarily-shaped pore: Mech. of Mat., 9, 165-179.

Dvorkin, J., Nur, A., and Yin, H., 1994, Effective properties of cemented granular material: Mech. of Mat., 12, 207-217.

Dvorkin, J. and Nur, A., 1996, Elasticity of high-porosity sandstones: Theory for two North Sea data sets: Geophysics, 61, 1363-1370.

Gassmann, F., 1951, Elasticity of porous media: Uber die elastizitat poroser medien: Vierteljahrsschrift der Naturforschenden Gesellschaft, 96, 1-23.

Hashin, Z., and Shtrikman, S., 1963, A variational approach to the elastic behavior of multiphase materials, J. Mech. Phys. Solids, 11, 127-140.

Nur, A.M., Marion, D. and Yin, H., 1991, Wave velocities in sediments, in: Shear Waves in Marine Sediments, J.M. Hovem et al., eds., Kluwer Academic Publishers.

Timoshenko, S.P., and Goodier, J.N., 1970, Theory of elasticity: McGraw-Hill.

Yin, H., 1993, Acoustic velocity and attenuation of rocks: Isotropy intrinsic anisotropy, and stress induced anisotropy: Ph.D. Thesis, Stanford University.

2.2. EFFECTIVE MODULI OF PARTICULATES WITH ELASTIC CEMENT

ABSTRACT

We give an approximate method for calculating the effective elastic moduli of a close random pack of identical elastic spheres whose pore space is partially or completely filled with elastic cement. To construct the solution we start with the uncemented pack and add small amounts of cement uniformly at every grain contact. The effective moduli of such an aggregate depend on those of the grains and cement (which are, generally, different), and on the amount of cement. Moduli for grain/cement mixtures are available from the contact cementation theory. Next we introduce an isotropic elastic body with void inclusions (e.g., spherical) whose porosity is the same as the porosity of the pack with contact cement. The moduli of the matrix are as yet unknown. We find them by assuming that the effective moduli of the elastic body with inclusions are equal to those of the pack with contact cement. Then an appropriate effective medium theory (e.g., self-consistent or differential effective medium approximation) provides two equations for the bulk and shear moduli of the matrix. Finally, we use the chosen effective medium theory to calculate the moduli of the elastic body with the matrix thus defined whose inclusions are now filled with the cement. We assume that these are also the moduli of the pack whose pore space is completely filled with the cement. To calculate the elastic moduli of the pack whose pore space is partially filled with the cement, we assume that they are those of the elastic body with the matrix thus defined and with two types of inclusions -- void and filled with cement. The porosities of this body and of the cemented pack are the same. This result gives one solution to a general and previously unresolved effective medium problem of contacting elastic inclusions embedded in an elastic matrix. It provides a transition from high-porosity cemented to completely cement-filled granular materials. The solution accurately predicts the compressional elastic modulus (the product of the bulk density and

P-wave velocity squared) from wave-propagation experiments on cemented glass beads and natural rocks.

INTRODUCTION AND PROBLEM FORMULATION

When estimating the effective stiffness of many composites, concrete and natural rock among them, one often faces the problem of calculating the moduli of an elastic matrix with elastic inclusions. This problem has been extensively addressed in the past. The existing solutions are analyzed and summarized by, e.g., Christensen (1991), Zimmerman (1991), Wang and Nur (1992), Nemat-Nasser and Hori (1993), and Berryman (1995). Accurate solutions are available for small inclusion concentrations and various inclusion shapes. To obtain an estimate for high concentrations, one may find the self-consistent (SC) or differential effective medium (DEM) approximations to be useful and reasonably accurate. Some fundamental solutions for composites with concentrated interacting inclusions belong to Frankel and Acrivos (1967), Goddard (1977), and Chen and Acrivos (1978).

An alternative to direct estimates is the bounding of the overall moduli of a composite (Hashin and Shtrikman, 1963). Nemat-Nasser et al. (1993) used generalized Hashin-Shtrikman variational principles to provide accurate bounds for composites with periodic microstructure. They also introduced a "modified equivalent inclusion method" for directly estimating the moduli of such composites. The results fall between the upper and lower bounds and are supported by experimental data on the shear modulus of an incompressible matrix reinforced by rigid spherical particles.

In composites with concentrated elastic inclusions, direct interaction between the inclusions through the thin layers of the matrix is very important (Goddard, 1977). The contact cementation theory (CCT) of Dvorkin et al. (e.g., 1994) highlights this conclusion. It allows one to calculate the effective elastic properties of a particulate aggregate where cement is located around the grain contacts (Figure 1a). CCT predicts that even small

volumes of contact cement (which may be soft as compared to the grains) act to strengthen the aggregate's elastic moduli, thus turning the nonlinear problem of contact analysis into a simpler linear one such as that found typically in composites analysis. The initial filling of the contact gaps is most important -- the effect of any additional cement placed around this initial filling is relatively small. This result is supported by experiments (Figure 2). Experiments also show that even by filling the entire pore space of a sphere pack one cannot achieve the drastic relative stiffness increase for which the small volumes of the contact cement are responsible.

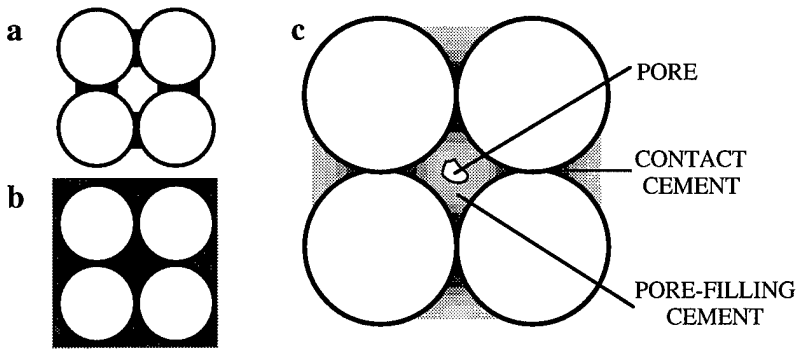

Figure 1. a. Grains with contact cement. b. Grains with pore space completely filled. c. Contact cement and pore-filling cement.

The assumptions used in CCT make its use appropriate only for high-porosity particulates where cement is located in the immediate vicinity of the contacts. As is, CCT cannot be used to estimate the elastic constants of a zero- or low-porosity aggregate where cement fills the whole pore space (Figure 1b) or large portions of it.

Therefore, a question naturally arises: How do we calculate the effective elastic moduli of particulates where cementation extends far beyond immediate grain-to-grain contacts? Consider, for example, a close random pack of identical glass beads where the pore space is completely filled with epoxy. This aggregate is a case of contacting spherical inclusions (glass) embedded in the epoxy matrix. From CCT we know that the filling (epoxy) located

at the contacts contributes most to the stiffness of the material. Then it is clear that a direct use of an inclusion theory (such as SC or DEM) is inappropriate here because it does not account for the special properties of cemented contacts. Contact cement and pore-filling cement (Figure 1c) contribute differently to the stiffness of the material.

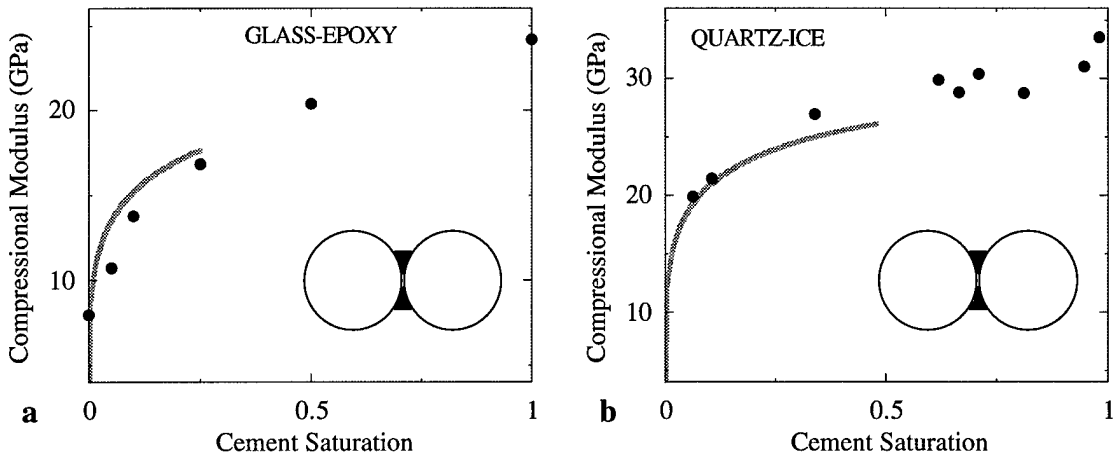

Figure 2. CCT theoretical predictions (curves) and experimental data (solid circles) for the compressional elastic modulus (the product of the bulk density and P-wave velocity squared) from elastic wave propagation experiments. The cemented samples were prepared by (a) adding epoxy to a close random pack of identical elastic spheres (Yin, 1993), and (b) adding water to Ottawa sand and then freezing it (Tutuncu et al., 1997). Both epoxy and water are wetting fluids and, when they solidify, act as contact cement in the form of pendular rings. The modulus is plotted versus the cement saturation of the pore space of the uncemented glass bead and sand packs.

To treat this problem our approach is to obtain a solution to the concentrated inclusion problem (the bulk and shear moduli of a close random pack of identical elastic spheres whose pore space is partially or completely filled with elastic cement) where the (previously ignored) special properties of the contact-cement part of the matrix are recognized and included. The problem posed is important, not only methodologically, because many cemented geomaterials, such as, e.g., asphalt concrete, have inclusion concentrations close to the upper limit, small void concentration (porosity) and large amounts of pore-filling cement.

SOLUTION

To solve this problem, we assume that at some high porosity where CCT is still applicable (Figure 3, point B), the effective bulk and shear moduli of the cemented material are those of a homogeneous isotropic matrix with empty spherical inclusions of the same porosity. Next we use an effective medium theory, for example, SC or DEM, to express these effective bulk and shear moduli through the, as yet unknown, elastic moduli of the hypothetical matrix material. Then the elastic moduli of the matrix material can be found from the two resulting equations.

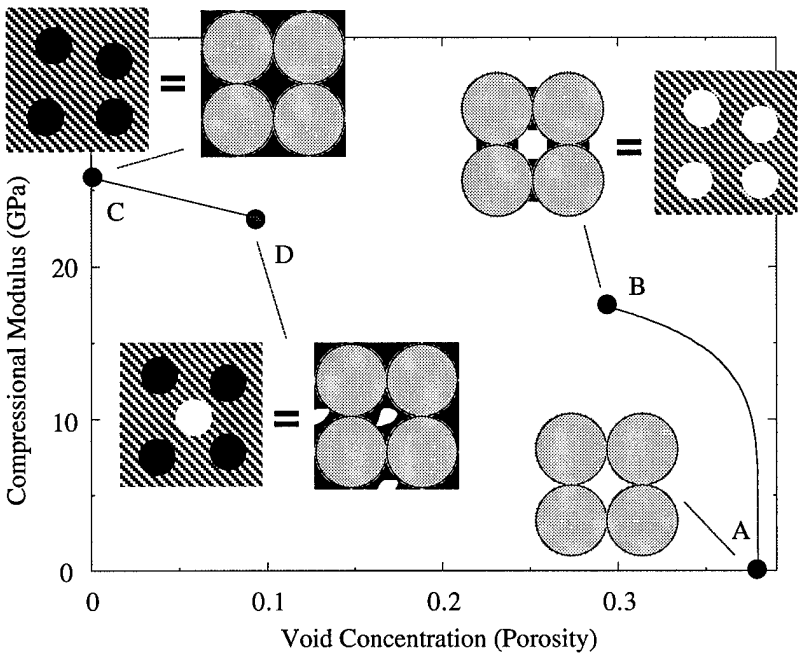

Figure 3. Proposed solution scheme. "A", uncemented sphere pack of zero stiffness. "B", pack with small volume of contact cement whose moduli are calculated from CCT; the moduli of the hypothetical matrix material are found from SC or DEM. "C", completely cemented matrix and sphere pack. "D", matrix and sphere pack of non-zero porosity. The graph (compressional modulus versus porosity) is given for epoxy-cemented glass beads.

To find the elastic moduli of the sphere pack where the entire pore space is filled with cement, we assume that they are the same as those of the hypothetical matrix whose

inclusions are now completely filled with the cement (Figure 3, point C). Those moduli can be computed using the chosen effective medium theory.

Finally, we find the moduli of the cemented sphere pack of a non-zero porosity by assuming that they are those of the cement-filled hypothetical matrix into which empty spherical inclusions are embedded (Figure 3, point D). The porosities of this new body with inclusions and of the cemented pack are the same. The mathematical expressions for this algorithm are given in Appendix.

Of course, the inclusions do not have to be spherical (results for ellipsoidal-shaped inclusions are easily obtained within the same approach), and effective medium theories other than SC and DEM could be used.

EXAMPLES

In the examples below, the compressional (M), bulk (K), and shear (G) moduli are calculated from the measured P- and S-wave velocities (V_p and V_s, respectively) and density ρ as $M = \rho V_p^2$, $G = \rho V_s^2$, $K = \rho(V_p^2 - 4V_s^2/3)$.

The wave-length in all the experiments is much larger that the individual grain size, which justifies the effective medium approach to the problem. Below, we use the compressional modulus instead of the bulk modulus because the former is calculated directly from V_p data which, generally, can be acquired with much higher accuracy than V_s data. The elastic properties of materials (glass, quartz, epoxy, and ice) used in the calculations are given in Table 1.

Table 1. Elastic moduli of materials used in calculations.

Material	M (GPa)	G (GPa)	K (GPa)
Glass	86	30.34	45.55
Epoxy	9.47	2	6.8
Quartz	96.6	45	36.6
Ice	13.27	3.53	8.57

Epoxy-Cemented Glass Beads. The elastic-wave velocities have been measured in glass bead packs cemented with epoxy (Yin, 1993). The porosity in these packs varied from zero in the fully-cemented pack to 0.38 in the uncemented pack. In its liquid state before solidification epoxy is a wetting fluid and tends to accumulate at the grain contacts. Therefore, at high porosities CCT is applicable to estimating the effective elastic moduli of cemented bead packs. We use this theory for porosities between 0.38 and 0.29. For porosities below 0.29 we use the above-described solution with SC (Berryman, 1980) and DEM (Norris, 1985; Zimmerman, 1991). Inclusions are spherical.

Our theoretical estimates match the experimental data for the compressional modulus extremely well (Figure 4) and overestimate the shear modulus (at least partially because CCT overestimates the shear modulus at high porosities). We cannot judge with certainty whether the poor prediction of the shear modulus is due to approximations used in CCT or to systematic errors in picking the S-wave first arrival in the experiments.

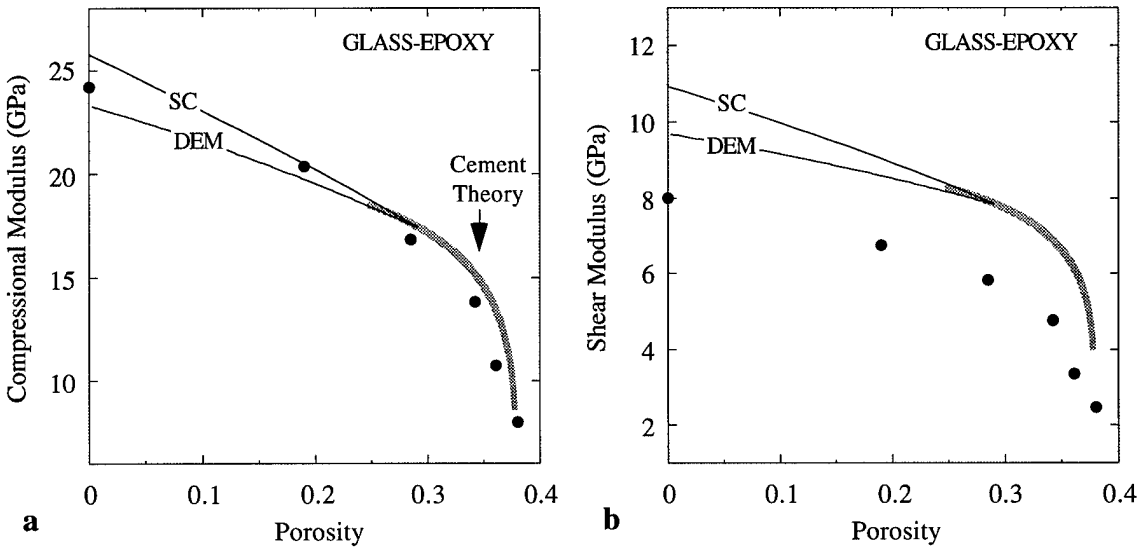

Figure 4. Theoretical (lines) and experimental (solid circles) values for the compressional (a) and shear (b) moduli of epoxy-cemented glass beads, plotted versus porosity. Bold lines are from CCT; thin lines are from the new solution.

An adjustable parameter in the solution is porosity above which CCT is used and below which the new solution is employed. The new solution is stable with respect to this parameter (as is shown in Figure 5) and, therefore, this transition porosity can be arbitrarily chosen within the reasonable limits where CCT is applicable.

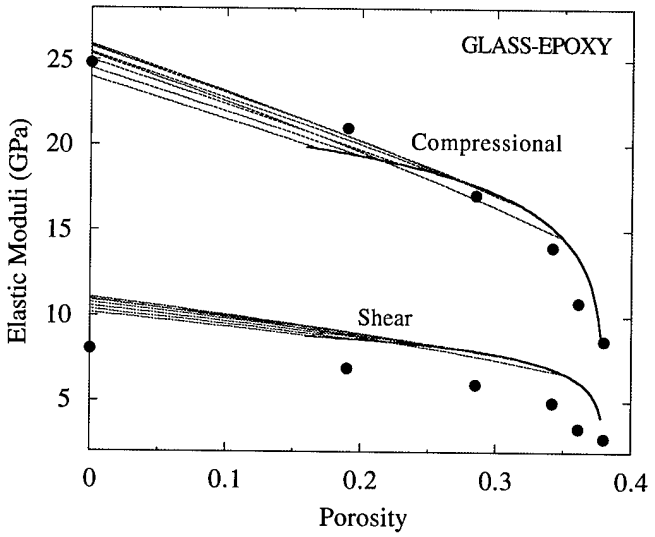

Figure 5. Stability of the new solution. Compressional and shear moduli of epoxy-cemented glass beads versus porosity. Bold lines are from CCT, thin lines are from the new solution (only SC is used in this example). They start at a varying transitional porosity. Solid circles are from the experiments.

It would be more satisfying if all of these curves intersected the zero porosity axis at the same modulus value, but instead we find that the present formulation of the theory produces a set of curves that are shifted (more or less) in parallel depending on their point of intersection with the CCT curve. This result suggests that the current formulation might be improved using a more sophisticated effective medium method. Further discussion of this point is in the Conclusion section of the paper.

Ice-Cemented Ottawa Sand. The elastic-wave velocities have been measured in partially-saturated and frozen pure-quartz Ottawa sand (Tutuncu et al., 1997). Similar to

the first example, our theoretical solution accurately models the experimental data for the compressional modulus and overestimates (as CCT does) the shear modulus (Figure 6).

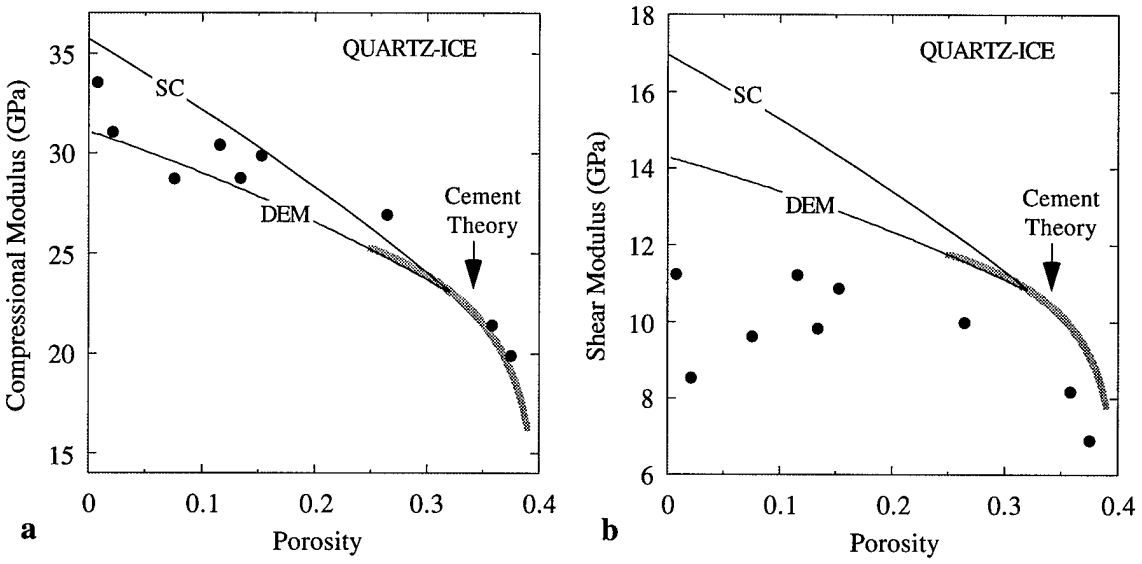

Figure 6. Theoretical (lines) and experimental (solid circles) values for the compressional (a) and shear (b) moduli of ice-cemented Ottawa sand, plotted versus porosity. Bold lines are from CCT, thin lines are from the new solution.

The high degree of scatter in the quartz-ice data (and especially so for the shear modulus) suggests that the role of crystalline ice in forming the microstructure of the cementing contacts between quartz grains is more complex (possibly due to the formation of polycrystalline ice) than in the other examples of cemented materials considered here.

Sintered Glass Beads. Elastic-wave velocity measurements were conducted on sintered glass beads by Berge et al. (1993). Berryman and Berge (1996) discuss the applicability of various effective medium theories to this dataset. Microphotographs show that the sintering resulted (because of glass melting) in glass pendular rings accumulated at the bead contacts. At the same time, microcracks are apparent in some beads. These

microcracks are likely to be the reason for the data scatter observed at high porosities (Figure 7). Still, the high-porosity data can be reasonably well mimicked by CCT.

The SC-based new solution matches the experimental data for the compressional modulus extremely well (Figure 7a). The DEM curve (Figure 4) underestimates it. Neither SC nor DEM curves match the shear modulus data but they do bracket it. In this case we have no doubts in the quality of the data because the datapoints approach the (independently measured) pure glass modulus as porosity approaches zero. We conclude that the new solution needs to be improved to better predict the shear modulus of a cemented aggregate.

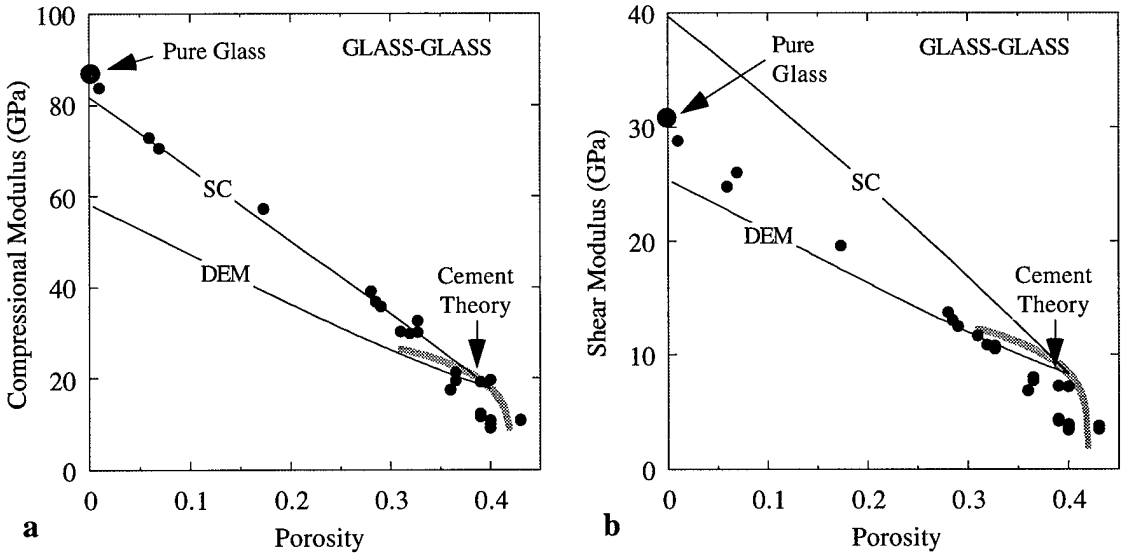

Figure 7. Theoretical (lines) and experimental (solid circles) values for the compressional (a) and shear (b) moduli of sintered glass beads, plotted versus porosity. Bold lines are from CCT, thin lines are from the new solution.

Natural Quartz Rocks. Many quartz rocks are created by diagenesis from beach sand. During diagenesis, quartz rims grow on the surfaces of the grains cementing them in the process. This cementation scheme is different from the pendular ring cementation because part of the cement is deposited on the grain surface away from the contacts. At the

same porosity, the contact cement volume and thus the rock's moduli are smaller than in the pendular ring case. Dvorkin and Nur (1996) apply CCT to predicting elastic moduli in high-porosity sandstones. The results match the data (Strandenes, 1991) well (Figure 8).

In order to model the medium- and low-porosity sandstone data (Han, 1986), we use CCT with the pendular-ring cementation. The datapoints tend to approach the SC-based new solution line as porosity approaches zero (Figure 8). What is most important, the theoretical results at zero porosity are close to the independently determined moduli of pure quartz. The DEM-based new solution underestimates these moduli.

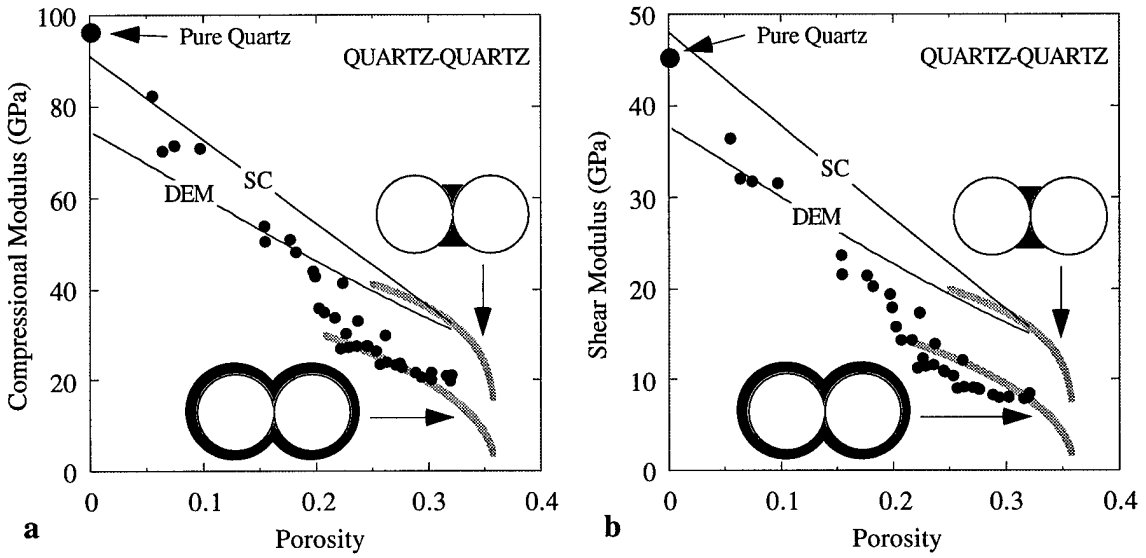

Figure 8. Theoretical (lines) and experimental (solid circles) values for the compressional (a) and shear (b) moduli of natural quartz rocks, plotted versus porosity. Bold lines are from CCT, thin lines are from the new solution. The CCT lines are plotted for two cementation schemes (as shown in the graphs): the pendular rings scheme and the cementing rims scheme.

CONCLUSION

We calculate the effective moduli of an elastic matrix with elastic inclusions at high concentration by modeling it as a cemented particulate aggregate. This approach allows us

to account for the important role of the contact cement part of the matrix and address the problem of **directly contacting inclusions**. The latter problem cannot be approached using traditional solutions where the inclusions are considered absolutely rigid (e.g., Frankel and Acrivos, 1967) and separated by a finite-thickness layer of the matrix.

The solution is a combination of the contact cementation theory and an effective medium theory such as the self-consistent or differential effective medium approximation. The solution is approximate because it uses a number of assumptions. Nevertheless, its predictions are confirmed by experimental data on cemented glass beads, sand, and natural rocks. The self-consistent approximation gives best results in the examples considered. We are able to accurately model the dynamic compressional moduli of these aggregates. At the same time, the errors in modeling the dynamic shear moduli may be as high as 25%. There may be at least two reasons for these errors: (a) commonly encountered inaccuracy in measuring elastic shear-wave velocity; and (b) theoretical errors in modeling the effective elastic modulus of a cemented high-porosity sphere pack. For the latter reason, additional effort is needed to improve our theoretical solution.

One legitimate criticism of the present formulation of the theory is that neither of the two effective medium theories used, although well-established and relatively easy to use, permits the user to control the microstructure of the resulting composite in any substantial way. In particular, both approaches when applied in Steps 3 and 4 (see Appendix) will surely violate our assumed microstructure for intermediate porosities by effectively placing voids in the grains (where we do not want them) as well as in the cement material (where we really do want them to be).

This effect will be comparatively small when the cementing material has similar or the same elastic parameters as the grains as is the case for our glass-glass and quartz-quartz examples. But it may have a substantial effect on the predicted properties in the cases

where the ratio of grain to cement properties is large as is the case for glass-epoxy and quartz-ice. The expected bias that would result from the undesired voids in the grains is that the predicted effective values of the grain/cement mixture at zero porosity must contain a higher proportion of grain material in the total volume than that present in the CCT calculations. The result will be a bias towards higher than realistic values at zero porosity and this is exactly what we observe for the SC theory in the glass-epoxy and quartz-ice examples. From this point of view, the present results should be considered preliminary; we need to continue searching for relatively simple effective medium theories that will permit us to gain control over the microstructure being modeled.

Still, this solution can be directly applied to estimating the stiffness of particulates such as asphalt concrete where the grains touch each other and the void fraction is small.

REFERENCES

Berge, P.A., Berryman, J.G., and Bonner, B.P., 1993, Influence of microstructure on rock elastic properties, Geophys. Res. Lett., 20, 2619-2622.

Berryman, J.G., 1980, Long-wavelength propagation in composite elastic media, I and II, J. Acoust. Soc. Amer., 68, 1809-1831.

Berryman, J.G., 1995, Mixture theories for rock properties, in Rock Physics and Phase Relations, T.J. Ahrens, ed., AGU Reference Shelf 3, AGU, Washington, DC., 205-228.

Berryman, J.G., and Berge, P.A., 1996, Critique of two explicit schemes for estimating elastic properties of multiphase composites, Mechanics of Materials, 22, 149-164.

Chen, H.-S., and Acrivos, A., 1978, The effective elastic moduli of composite materials containing spherical inclusions at non-dilute concentrations, Int. J. Solids Structures, 14, 349-361.

Christensen, R.M., 1991, Mechanics of Composite Materials, Krieger Publishing Company, Malabar, Florida.

Dvorkin, J., Nur, A. and Yin, H., 1994, Effective properties of cemented granular material, Mechanics of Materials, 18, 351-366.

Dvorkin, J., and Nur, A., 1996, Elasticity of high-porosity sandstones: Theory for two north sea datasets, Geophysics, 61, 1363-1370.

Frankel, N.A., and Acrivos, A., 1967, On the viscosity of a concentrated suspension of solid spheres, Chem. Eng. Sci., 22, 847-853.

Goddard, J.D., 1977, An elastodynamic theory for the rheology of concentrated suspensions of deformable particles, Proc. R. Soc. Lond., A 430, 105-131.

Han, D.-H., 1986, Effects of porosity and clay content on acoustic properties of sandstones and unconsolidated sediments: Ph.D. thesis, Stanford University.

Hashin, Z., and Shtrikman, S., 1963, A variational approach to the elastic behavior of multiphase materials: J. Mech. Phys. Solids, 11, 127-140.

Nemat-Nasser, S., and Hori, M., 1993, Micromechanics: Overall Properties of Heterogeneous materials, North-Holland, Amsterdam.

Nemat-Nasser, S., Yu, N., and Hori, M., 1993, Bounds and estimates of overall moduli of composites with periodic microstructure, Mechanics of Materials, 15, 163-181.

Norris, A.N., 1985, A differential scheme for the effective moduli of composites, Mechanics of Materials, 4, 1-16.

Strandenes, S., 1991, Rock physics analysis of the Brent Group Reservoir in the Oseberg Field: Stanford Rock Physics and Borehole Geophysics Project.

Tutuncu, A.N., Dvorkin, J., and Nur, A., 1997, Elastic-wave velocities in frozen Ottawa sand, Geophys. Res. Lett., in press.

Wang, Z., and Nur, A. (eds.), 1992, Seismic and Acoustic Velocities in Reservoir Rocks, 2, SEG, Tulsa, Oklahoma.

Yin, H., 1993, Acoustic Velocity and Attenuation of Rocks: Isotropy, Intrinsic Anisotropy, and Stress Induced Anisotropy, Ph.D. thesis, Stanford University.

Zimmerman, R.W., 1991, Compressibility of Sandstones, Elsevier, Amsterdam.

APPENDIX: SOLUTION ALGORITHM

Step 1, Contact Cementation Theory (CCT). The effective compressional (M_{CCT}), bulk (K_{CCT}), and shear (G_{CCT}) moduli of a random dense pack of identical spheres cemented at their contacts are (Dvorkin and Nur, 1996):

$$K_{CCT} = \frac{n(1-\phi_0)}{6} M_c S_n, \quad G_{CCT} = \frac{3}{5} K_{CCT} + \frac{3n(1-\phi_0)}{20} G_c S_\tau, \quad M_{CCT} = K_{CCT} + \frac{4}{3} G_{CCT};$$

where M_c and G_c are the compressional and shear moduli of the cement respectively; $\phi_0 \approx 0.36$ is the porosity of the uncemented pack; and $n \approx 8.5$ is the average number of contacts per grain.

Parameters S_n and S_τ are:

$$S_n = A_n(\Lambda_n)\alpha^2 + B_n(\Lambda_n)\alpha + C_n(\Lambda_n),\ A_n(\Lambda_n) = -0.024153 \cdot \Lambda_n^{-1.3646},$$
$$B_n(\Lambda_n) = 0.20405 \cdot \Lambda_n^{-0.89008},\ C_n(\Lambda_n) = 0.00024649 \cdot \Lambda_n^{-1.9864};$$
$$S_\tau = A_\tau(\Lambda_\tau, \nu)\alpha^2 + B_\tau(\Lambda_\tau, \nu)\alpha + C_\tau(\Lambda_\tau, \nu),$$
$$A_\tau(\Lambda_\tau, \nu) = -10^{-2} \cdot (2.26\nu^2 + 2.07\nu + 2.3) \cdot \Lambda_\tau^{0.079\nu^2 + 0.1754\nu - 1.342},$$
$$B_\tau(\Lambda_\tau, \nu) = (0.0573\nu^2 + 0.0937\nu + 0.202) \cdot \Lambda_\tau^{0.0274\nu^2 + 0.0529\nu - 0.8765},$$
$$C_\tau(\Lambda_\tau, \nu) = 10^{-4} \cdot (9.654\nu^2 + 4.945\nu + 3.1) \cdot \Lambda_\tau^{0.01867\nu^2 + 0.4011\nu - 1.8186};$$
$$\Lambda_n = \frac{2G_c}{\pi G} \frac{(1-\nu)(1-\nu_c)}{1-2\nu_c},\ \Lambda_\tau = \frac{G_c}{\pi G};$$

where G and ν are the shear modulus and the Poisson's ratio of the grain material, respectively; and ν_c is the Poisson's ratio of the cement. Parameter α depends on the contact cementation scheme. It is

$$\alpha = 2\left[\frac{\phi_0 - \phi}{3n(1-\phi_0)}\right]^{0.25}$$

for the pendular ring scheme and

$$\alpha = \left[\frac{2(\phi_0 - \phi)}{3(1-\phi_0)}\right]^{0.5}$$

for the scheme where the surface of a grain is evenly covered with the cement rim. ϕ is the porosity of the cemented aggregate which is smaller than ϕ_0 because of cement deposited in the pore space of the sphere pack.

Step 2, Self-Consistent Approximation (SC). If the moduli K_s and G_s of the hypothetical matrix material were known, then the self-consistent approximation for spherical inclusions of void with concentration ϕ predicts that K_{CCT} and G_{CCT} are given by the coupled equations (Berryman, 1980):

$$\frac{1}{K_{CCT}+\frac{4}{3}G_{CCT}}=\frac{1-\phi}{K_s+\frac{4}{3}G_{CCT}}+\frac{\phi}{\frac{4}{3}G_{CCT}},$$

$$\frac{1}{G_{CCT}+Z}=\frac{1-\phi}{G_s+Z}+\frac{\phi}{Z},\quad Z=\frac{G_{CCT}(9K_{CCT}+8G_{CCT})}{6(K_{CCT}+2G_{CCT})}.$$

These equations have to be solved iteratively to find K_{CCT} and G_{CCT} when K_s and G_s are known. But, since K_{CCT} and G_{CCT} are already given in Step 1, we may solve the two equations instead for K_s and G_s. Solving in this direction, the equations decouple and provide explicit, unique results for K_s and G_s.

Step 2', Differential Effective Medium Approximation (DEM). In this case K_s and G_s can be found from the following two equations (Norris, 1985):

$$\frac{G_{CCT}}{G_s}=(1-\phi)^2\left[\frac{1.5+\lambda_s G_{CCT}/G_s}{1.5+\lambda_s}\right]^{\frac{1}{3}},\quad \frac{K_{CCT}}{K_s}=\frac{G_{CCT}}{G_s}\frac{0.75+\lambda_s}{0.75+\lambda_s(G_{CCT}/G_s)^{\frac{3}{5}}};$$

where

$$\lambda_s=\frac{3(1-5\nu_s)}{4(1+\nu_s)},\quad \nu_s=\frac{1}{2}\frac{3K_s-2G_s}{3K_s+G_s}.$$

Norris' result can be rewritten to show explicitly that

$$\lambda_s=\lambda_{CCT}(1-\phi)^{-\frac{6}{5}}\left(\frac{1.5+\lambda_s}{1.5+\lambda_{CCT}}\right)^{\frac{1}{5}},$$

where

$$\lambda_{CCT} = \frac{3(1-5\nu_{CCT})}{4(1+\nu_{CCT})}, \quad \nu_{CCT} = \frac{1}{2}\frac{3K_{CCT}-2G_{CCT}}{3K_{CCT}+G_{CCT}}.$$

Although this is an implicit equation relating λ_s to λ_{CCT} (and therefore must be solved iteratively), we can see that the equation is "almost" explicit by noting that $\nu_{CCT} \approx 0.2$ is often a good approximation for porous media. Then both λ_s and λ_{CCT} will be small in magnitude and, therefore, the last factor in the right-hand side of the equation will be closely approximated by unity. Thus λ_s is uniquely determined by λ_{CCT} and ϕ in the expected range of the elastic parameters for porous materials.

Step 3 and 4, SC. The moduli K_{Fill} and G_{Fill} of the matrix where all inclusions (of concentration ϕ) are filled with the cement can be found from the following two equations (Berryman, 1980):

$$(1-\phi)(K_s - K_{Fill})P_s + \phi(K_c - K_{Fill})P_c = 0,$$
$$(1-\phi)(G_s - G_{Fill})Q_s + \phi(G_c - G_{Fill})Q_c = 0,$$

where

$$P_s = \frac{K_{Fill}+\frac{4}{3}G_{Fill}}{K_s+\frac{4}{3}G_{Fill}}, \quad P_c = \frac{K_{Fill}+\frac{4}{3}G_{Fill}}{K_c+\frac{4}{3}G_{Fill}},$$
$$Q_s = \frac{G_{Fill}+Z}{G_s+Z}, \quad Q_c = \frac{G_{Fill}+Z}{G_c+Z}, \quad Z = \frac{G_{Fill}(9K_{Fill}+8G_{Fill})}{6(K_{Fill}+2G_{Fill})}.$$

Next we calculate the effective moduli (K_{Eff} and G_{Eff}) of the same matrix where some of the inclusions are filled with the cement, and some are empty. If the concentration of the empty inclusions is ϕ_e, the concentration of the cemented inclusions is $\phi - \phi_e$ because the volumetric fraction of the matrix is still $1-\phi$. The desired moduli are found from the following two equations:

$$(1-\phi)(K_s - K_{Eff})P_s + (\phi-\phi_e)(K_c - K_{Eff})P_c - \phi_e K_{Eff} P_0 = 0,$$
$$(1-\phi)(G_s - G_{Eff})Q_s + (\phi-\phi_e)(G_c - G_{Eff})Q_c - \phi_e G_{Eff} Q_0 = 0,$$

where

$$P_s = \frac{K_{Eff} + 4/3 G_{Eff}}{K_s + 4/3 K_{Eff}}, \quad P_c = \frac{K_{Eff} + 4/3 G_{Eff}}{K_c + 4/3 G_{Eff}}, \quad P_0 = \frac{K_{Eff} + 4/3 G_{Eff}}{4/3 G_{Eff}},$$

$$Q_s = \frac{G_{Eff} + Z}{G_s + Z}, \quad Q_c = \frac{G_{Eff} + Z}{G_c + Z}, \quad Q_0 = \frac{G_{Eff} + Z}{Z}, \quad Z = \frac{G_{Eff}(9K_{Eff} + 8G_{Eff})}{6(K_{Eff} + 2G_{Eff})}.$$

Steps 3' and 4', DEM. We use the iterative scheme developed by Norris (1985). We choose a volumetric fraction increment $d\phi$ such that $d\phi << \phi$. The total number of iterations N is (Zimmerman, 1991):

$$N = -\frac{\ln(1-\phi)}{d\phi}.$$

The number of the first N_e steps is $N_e = N\phi_e / \phi$. During these iterations we calculate the effective bulk K_{Eff} and shear G_{Eff} moduli as:

$$K_{Eff}^{(j+1)} = K_{Eff}^{(j)} - \frac{K_{Eff}^{(j)}(4G_{Eff}^{(j)} + 3K_{Eff}^{(j)})}{4G_{Eff}^{(j)}} d\phi,$$

$$G_{Eff}^{(j+1)} = G_{Eff}^{(j)} - \frac{G_{Eff}^{(j)}(15K_{Eff}^{(j)} + 20G_{Eff}^{(j)})}{9K_{Eff}^{(j)} + 8G_{Eff}^{(j)}} d\phi;$$

$$K_{Eff}^{(0)} = K_s, \quad G_{Eff}^{(0)} = G_s.$$

The last $N - N_e$ iterations are performed using equations

$$K_{Eff}^{(j+1)} = K_{Eff}^{(j)} + \frac{(K_c - K_{Eff}^{(j)})(4G_{Eff}^{(j)} + 3K_{Eff}^{(j)})}{4G_{Eff}^{(j)} + 3K_c} d\phi,$$

$$G_{Eff}^{(j+1)} = G_{Eff}^{(j)} + \frac{(G_c - G_{Eff}^{(j)})(15K_{Eff}^{(j)} + 20G_{Eff}^{(j)})}{9K_{Eff}^{(j)} + 8G_{Eff}^{(j)} + 6(K_{Eff}^{(j)} + 2G_{Eff}^{(j)})G_c / G_{Eff}^{(j)}} d\phi.$$